Schiff-Base Cross-Linked Hydrogels Based on Properly Synthesized Poly(ether urethane)s as Potential Drug Delivery Vehicles in the Biomedical Field: Design and Characterization

ACS OMEGA

Open Access

http://pubs.acs.org/journal/acsodf

Article

Schiff-Base Cross-Linked Hydrogels Based on Properly Synthesized Poly(ether urethane)s as Potential Drug Delivery Vehicles in the Biomedical Field: Design and Characterization

Roberta Pappalardo,[⊥] Monica Boffito,*[,⊥] Claudio Cassino, Valeria Caccamo, Valeria Chiono, and Gianluca Ciardelli*

Cite This: *ACS Omega* 2024, 9, 45774−45788

Read Online

ACCESS | Metrics & More | Article Recommendations | Supporting Information

ABSTRACT: *In situ*-forming hydrogels based on the Schiff-base chemistry are promising for drug delivery applications, thanks to their stability under physiological conditions, injectability, self-healing properties, and pH-responsiveness. In this work, two water-soluble poly(ethylene glycol)-based poly(ether urethane)s (PEUs) were engineered. A high-molecular-weight PEU (SHE3350, $\bar{M}_n$ 24 kDa, *D* 1.7), bearing primary amino groups along each polymeric chain, was synthesized using N-Boc serinol and subjected to an acidic treatment to expose primary amines (*ca.* 10^{20} units/$g_{SHE3350}$). In parallel, a low-molecular-weight PEU (AHE1500, $\bar{M}_n$ 4 kDa, *D* 1.5) with aldehyde end groups was synthesized by end-capping an isocyanate-terminated prepolymer with 4-hydroxybenzaldehyde, and the aldehyde groups were quantified to be around 10^{20} units/$g_{AHE1500}$. Hydrogels were prepared by simply mixing SHE3350 and AHE1500 aqueous solutions and characterized to assess their physico-chemical and rheological properties. Schiff-base bond formation was proved through carbon-13 and proton solid-state NMR spectroscopies. Rheological characterization confirmed the formation of gels with high resistance to applied strain (*ca.* 1000%). Hydrogels exhibited high absorption ability (*ca.* 270% increase in wet weight) in physiological-like conditions (i.e., 37 °C and pH 7.4) up to 27 days. In contact with buffer at pH 5, enhanced fluid absorption was observed until dissolution occurred starting from 13 days due to Schiff-base hydrolysis in acidic conditions. Conversely, gels showed a reduced absorption ability at pH 9 due to shrinkage phenomena. Furthermore, they exhibited high permeability and controlled, sustained, and pH-triggered release of a model molecule (i.e., fluorescein isothiocyanate dextran) for up to 17 days. Lastly, the hydrogels showed easy injectability and self-healing ability.

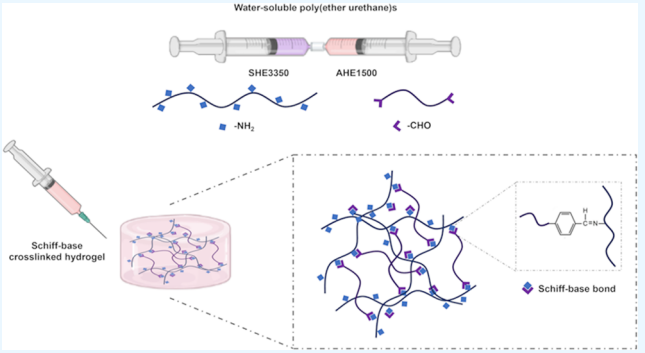

1. INTRODUCTION

Hydrogels are three-dimensional (3D) hydrophilic polymeric networks able to absorb and retain a considerable amount of water or biological fluids without dissolving due to the presence of cross-links between the polymer chains.[1] Besides their biocompatibility, hydrogels often exhibit easy injectability and extrusion. For these reasons, they have been extensively researched for tissue engineering (TE) applications as their high water content provides a physiologically similar environment to the native extracellular matrix (ECM). Furthermore, the capability of encapsulating and transferring their payload to the surrounding tissues allows the delivery of therapeutic agents (e.g., drugs or biomolecules) or cells to the target site in a minimally invasive manner.[2−4] As drug delivery systems, injectable hydrogels have been developed to improve drug bioavailability and prolong drug release, thus minimizing side effects and providing a sustained *in situ* release.[5,6] Starting from the precursor solution containing the therapeutic agents, injectable hydrogels can be obtained through different strategies, depending on the physical or chemical cross-linking reactions that drive their *in situ* sol-to-gel transition.[7] The gelation of physically cross-linked hydrogels is driven by non-covalent interactions occurring between the polymer chains, and gel formation does not require the addition of cross-linking agents or catalysts.[8] For this reason, physical injectable hydrogels are easy to fabricate and highly biocompatible, and they ensure payload integrity during the sol-to-gel transition. However, their reversible nature is generally accompanied by low reactivity, slow response time in their formation, and poor stability.[9] Conversely, chemical injectable hydrogels result from

Received: April 2, 2024
Revised: July 9, 2024
Accepted: August 2, 2024
Published: November 7, 2024

the formation of covalent bonds between the polymer chains. Usually, chemically cross-linked hydrogels show high reactivity, good stability under physiological conditions, and superior mechanical properties compared to physically cross-linked systems.[10,11] Nevertheless, the possible adverse effects associated with the use of toxic cross-linking agents or initiators needed for some of these cross-linking reactions represent the main limitation.[12] In the plethora of chemical hydrogels, great efforts have recently been dedicated to developing hydrogels based on Schiff-base linkages since they exhibit the main pros of chemical hydrogels (i.e., fast gelation and favorable stability under physiological conditions) without any toxic chemical cross-linking agent required for their preparation. Indeed, these chemical hydrogels are based on the Schiff-base chemistry, which consists of the reversible condensation reaction between a primary amine ($-NH_2$) and an aldehyde group (−CHO), forming a dynamic covalent bond (−C═N), known as the imine bond, belonging to the class of Schiff-bases.[13,14] The characteristic reversibility of Schiff-base bonds makes them interesting for the design of dynamic hydrogels.[15] Indeed, they behave as covalent chemically stable cross-linked hydrogels, but they are also able to recover their network after bond breakage, even in response to an external stimulus. This feature confers intriguing properties to these hydrogels, such as injectability and self-healing ability.[16−19] Moreover, the literature also reports about their pH-responsiveness, which is an interesting feature to exploit for designing pH-triggered drug release systems.[20−23] In this scenario, in the last years, our research group has gained experience in engineering *in situ*-forming physically cross-linked injectable hydrogels as potential drug delivery systems by exploiting the versatility of poly(ether urethane)s (i.e., PEUs) as constituent materials. In particular, it has been demonstrated that micellar thermosensitive hydrogels, designed starting from PEUs based on Poloxamer P407 (i.e., poly(ethylene oxide)−poly(propylene oxide)−poly(ethylene oxide)—PEO−PPO−PEO—copolymer) as macrodiol,[24] allow the encapsulation of drugs with different wettabilities.[25] In addition, it has been proved that PEUs can be chemically modified using multiple functionalization techniques to provide thermo-responsive hydrogels with additional sensitivity to external stimuli (e.g., pH and UV/vis light).[26,27] Lastly, the spontaneous self-assembly of PEU polymeric chains and α-cyclodextrins (i.e., α-CDs) into poly(pseudo)rotaxane crystals was recently investigated to engineer supramolecular hydrogels as drug delivery vehicles.[28,29] Starting from this evidence, in this work, we engineered new PEU-based chemically cross-linked injectable hydrogels by exploiting the Schiff-base chemistry, with the aim to design *in situ*-forming hydrogels for sustained drug release. To achieve this purpose, two water-soluble PEUs with suitable molecular weight and a significant amount of functionalities (i.e., a high-molecular-weight PEU exposing $-NH_2$ groups and a −CHO bearing low-molecular-weight PEU) were synthesized according to optimized protocols. Specifically, PEUs were synthesized starting from poly(ethylene glycol) (i.e., PEG) as macrodiol, 1,6-hexamethylene diisocyanate (i.e., HDI) as diisocyanate, and N-Boc serinol or 4-hydroxybenzaldehyde as chain extender and end-capping molecule, respectively. The two PEUs were thoroughly chemically characterized by infrared (IR) and nuclear magnetic resonance (NMR) spectroscopies, size exclusion chromatography, and colorimetric assays. Then, their aqueous solutions were mixed to formulate chemically cross-linked hydrogels, resulting from the formation of Schiff-base bonds between primary amino groups exposed along the polymer chains and aldehyde end groups. Hydrogels were chemically characterized by IR and solid-state NMR spectroscopies to assess the presence of imine covalent cross-links between the PEU chains. Then, the gelation time and rheological properties were investigated. Their behavior in aqueous environments at different pH conditions was evaluated up to 27 days. Furthermore, to prove their potential as drug delivery systems, the release profile of a model molecule (i.e., fluorescein isothiocyanate dextran) was studied at different pH conditions. Lastly, injectability and self-healing ability were qualitatively evaluated. To the best of our knowledge, we report for the first time the formulation of hydrogels based on imine bonds starting from *ad hoc* synthesized poly(ether urethane)s exposing primary amines and aldehyde groups. We successfully exploited the versatility of poly(urethane) chemistry to confer highly tunable physicochemical properties to the developed hydrogels. Furthermore, the use of solid-state nuclear magnetic resonance spectroscopy is reported as a promising tool to chemically assess the formation of imine bonds among the polymeric chains.

2. MATERIALS AND METHODS

2.1. Materials for Poly(ether urethane) Synthesis. Poly(ethylene glycol) (PEG3350, $\overline{M}_n$ 3350 Da, PEG1500, $\overline{M}_n$ 1500 Da), 1,6-hexamethylene diisocyanate (HDI), dibutyltin dilaurate (DBTDL), and N-Boc-serinol (N-Boc) were purchased from Sigma-Aldrich, Milano, Italy. 4-hydroxybenzaldehyde (BA) was purchased from TCI Chemicals, Zwijndrecht, Belgium. All reagents were dried before use: PEG3350 and PEG1500 were dehydrated for 8 h at 100 °C under vacuum conditions (*ca.* 200 mbar pressure) and then equilibrated at 30 °C under vacuum; HDI was distilled under low pressure to remove moisture and stabilizers; N-Boc was dried overnight under vacuum at room temperature, while BA was stored under vacuum and inert atmosphere until use. Tetrahydrofuran (THF, Thermo Fisher, Kandel, Germany) was used as a solvent for PEU synthesis; before use, it was dried over activated molecular sieves (4 Å, Sigma-Aldrich, Milano, Italy) under a N_2 atmosphere overnight. All other solvents were purchased from Carlo Erba Reagents, Milano, Italy, in analytical grade and used as received.

2.2. Synthesis of Poly(ether urethane) Bearing Primary Amino Groups. A water-soluble PEU, referred to by the acronym NHE3350, was synthesized through an optimized one-step synthesis procedure by selecting PEG3350 as macrodiol, HDI as diisocyanate, and N-Boc as chain extender. Briefly, PEG3350 was melted at 70 °C and subjected to four vacuum-inert gas cycles, each cycle consisting of 4 min at low pressure (around 3−4 mbar) followed by a N_2 inflow for 2 min. N-Boc (1:1 molar ratio with respect to PEG3350) was solubilized in anhydrous THF at 5% (w/v) and added. Then, HDI and DBTDL as catalyst were, respectively, added at a 1:1 molar ratio and 0.1% w/w with respect to PEG3350 and N-Boc. The reaction was carried on under stirring for 10 min at 70 °C. Subsequently, the system was cooled down at room temperature, and the reaction was stopped by adding methanol (MeOH) (6 mL of MeOH/16 g of theoretically synthesized PEU) to passivate any residual isocyanate group. Anhydrous THF was also added at 20% (w/v) to solubilize the synthesized PEU and facilitate its recovery.

https://doi.org/10.1021/acsomega.4c03157
ACS Omega 2024, 9, 45774−45788

NHE3350 was collected by precipitation in petroleum ether (4:1 v/v ratio with respect to THF) under vigorous stirring. Finally, the PEU was separated from the supernatant and dried overnight in a fume hood. Then, the PEU was again solubilized in THF (30% w/v) and purified in diethyl ether (DEE) (5:1 v/v ratio with respect to THF). The precipitated PEU was separated, dried overnight under the fume hood, and stored under vacuum conditions until use. To assess the repeatability of the synthesis process, three different batches were synthesized.

2.3. Primary Amine Exposure. NHE3350 was subjected to an acidic treatment to remove Boc protecting groups, thus exposing primary amines, according to the procedure published by Boffito et al. with some modifications.[30] Briefly, 2 g of PEU were dissolved in 40 mL of chloroform for 2 h, at room temperature (RT), under magnetic stirring (250 rpm) and N_2 flow. Then, 10 mL of trifluoroacetic acid (TFA, Sigma-Aldrich, Milano, Italy) were added and the reaction proceeded for 1 h. To remove the solvent, the PEU solution was concentrated in a rotary evaporator (Buchi Rotavapor Labortechnik AG, Switzerland) and washed twice with 20 mL of chloroform. The deprotected PEU, referred to as SHE3350, was dissolved in 40 mL of deionized water overnight. Lastly, SHE3350 solution was dialyzed (12−14 kDa cutoff membrane, Sigma-Aldrich, Milano, Italy) for 1 week against deionized water and filtered using a Buchner system to remove Boc groups, residual solvent, and impurity traces and then freeze-dried (Martin Christ Alpha 2−4 LSC instrument, Germany). To assess the deprotection protocol's repeatability, three different samples were subjected to the same treatment.

2.4. Chemical Characterization of NHE3350 and SHE3350 Poly(ether urethane)s. *2.4.1. Attenuated Total Reflectance-Fourier Transform Infrared (ATR-FTIR) Spectroscopy.* To prove the successful NHE3350 synthesis and to ensure the presence of the characteristic urethane bonds even after the deprotection process, ATR-FTIR spectroscopy was performed using a PerkinElmer Spectrum 100 equipped with an ATR accessory (UATR KRSS) with a diamond crystal. NHE3350 and SHE3350 were analyzed at RT in the spectral range of 4000−600 cm^{-1} (resolution 4 cm^{-1}, 32 scans). As a reference, the PEG3350 spectrum was also registered according to the same protocol. The recorded spectra were analyzed and compared using the PerkinElmer Spectrum Software.

2.4.2. Size Exclusion Chromatography (SEC). PEU molecular weight distribution profile was assessed using an Agilent Technologies 1200 Series (California, United States) instrument equipped with a refractive index detector (RID) and two Waters Styragel columns (HR1 and HR4) equilibrated at 55 °C. *N*,*N*-Dimethylformamide (DMF, HPLC grade, Carlo Erba Reagents, Milano, Italy), added with 0.1% w/v LiBr (Sigma-Aldrich, Milano, Italy), was used as the mobile phase. Before analysis, 2 mg of PEU were dissolved in 1 mL of mobile phase and filtered through a 0.45 μm poly(tetrafluoroethylene) (PTFE) syringe filter (LLG International, Meckenheim, Germany). The number-average molecular weight ($\overline{M}_n$), weight-average molecular weight ($\overline{M}_w$), and polydispersity index (D) were estimated using the Agilent ChemStation Software by referring to a calibration curve based on poly(ethylene oxide) (PEO) standards with a peak molecular weight M_p ranging between 982 and 205,500 Da.

2.4.3. Proton Nuclear Magnetic Resonance (^{1}H NMR) Spectroscopy. ^{1}H NMR spectroscopy was performed by using a Bruker Avance NEO spectrometer (Bruker Biospin AG, Fällanden, Switzerland) equipped with an 11.75 T superconducting magnet (500 MHz ^{1}H Larmor frequency) and a Bruker multinuclear SMARTProbe probe. Samples were prepared by solubilizing 10 mg of NHE3350 and SHE3350 in 0.75 mL of deuterium oxide (D_2O, 99.8%, Sigma-Aldrich, Milano, Italy). The NMR spectra were obtained as the average of 24 scans, with a 3.5 s relaxation time. The resulting spectra were elaborated using MNova software (Mestrelab Research, S.L, Spain). As a control, the ^{1}H NMR of N-Boc-serinol was also recorded according to the same protocol.

2.4.4. Quantification of Exposed Primary Amines through Colorimetric Assay. The primary amino groups exposed along the SHE3350 polymer backbone were quantified through the Orange II Sodium Salt (Sigma-Aldrich, Milano-Italy) colorimetric assay.[31] Briefly, 20 mg of SHE3350 were dissolved in 50 mL of a 0.175 mg/mL Orange II Sodium Salt aqueous solution adjusted at pH 3 using 1 M HCl. The reversible electrostatic interactions between the cationic SHE3350 and the anionic dye molecules were allowed to form for 18 h at RT in the dark. In order to remove the unbound dye molecules, samples were dialyzed (3500 Da cutoff membrane, Spectrum Spectra/Por 4) against ultrapure water for 1 week with two refreshes per day and finally freeze-dried (Martin Christ Alpha 2−4 LSC instrument, Germany). The same procedure was also performed on the NHE3350 polymer to assess the occurrence of adsorption phenomena of dye molecules to the poly(ether urethane) backbone. After freeze-drying of both SHE3350 and NHE3350 samples, 10 mg of lyophilized polymer were solubilized in 1 mL of an aqueous solution adjusted at pH 12 with 1 M NaOH. The desorption reaction of the grafted or simply adsorbed dye molecules was carried on for 2 h at RT in the dark. Then, sample absorbance was measured with a UV−visible spectrophotometer (PerkinElmer, Lambda 365) in the spectral range of 700−300 nm, and the primary amines were quantified by referring to a calibration curve based on Orange II Sodium Salt aqueous solutions at pH 12 with defined concentrations (ranging between 2.188 and 21.875 μg/mL). Tests were conducted in triplicate and reported as the average ± standard deviation.

2.5. Synthesis of Poly(ether urethane) with Aldehyde End Groups. The water-soluble PEU, referred to by the acronym AHE1500, was synthesized by selecting PEG1500, HDI, and BA as building blocks. AHE1500 was synthesized by end-capping an isocyanate-terminated prepolymer, according to a modified version of a protocol reported in the literature.[32] Specifically, PEG1500 was pretreated as mentioned above and solubilized in anhydrous THF (30% w/v concentration) at 60 °C. HDI and DBTDL were added at a 2.1:1 molar ratio and 0.1% (w/w) with respect to PEG1500, respectively. Then, the first step of the synthesis was conducted for 30 min. In the second step, BA was added (13% w/v in THF, 2.1:1 molar ratio with respect to PEG1500) and the reaction was carried on for 2.5 h at 60 °C. Finally, the reaction was stopped with MeOH and AHE1500 was collected and purified as previously described. The PEU was stored under an inert atmosphere at 4 °C until use. To assess the synthesis process repeatability, three different PEU batches were synthesized.

2.6. Chemical Characterization of AHE1500 Poly(ether urethane). *2.6.1. ATR-FTIR Spectroscopy and SEC Analysis.* Both ATR-FTIR spectroscopic and SEC analyses were performed to characterize AHE1500 and assess its successful production. AHE1500, BA, and PEG1500 ATR-

https://doi.org/10.1021/acsomega.4c03157
ACS Omega 2024, 9, 45774−45788

FTIR spectra were recorded as mentioned above. In addition, the number-average molecular weight ($\overline{M_n}$), weight-average molecular weight (M_w), and polydispersity index (D) were estimated according to the protocol described in Section 2.4.2.

2.6.2. ^{1}H NMR Spectroscopy and Quantification of Aldehyde Groups by UV−Visible Spectroscopy. The successful synthesis of AHE1500 was also verified by ^{1}H NMR spectroscopy according to the previously described method with a slight modification. Samples were prepared by dissolving AHE1500 and BA (as control) in deuterated dimethyl sulfoxide (d_6-DMSO, 99.8% D with 0.03% TMS, Sigma-Aldrich, Milano, Italy) at 1.3% w/v concentration. Moreover, to quantify the number of exposed aldehyde groups, UV−visible spectroscopy was conducted by measuring the absorbance of the benzaldehyde group at 285 nm. Briefly, 10 mg of AHE1500 were dissolved in 2 mL of ultrapure water. Aldehyde groups were quantified by referring to a calibration curve based on BA molecule aqueous solutions with defined concentrations (ranging between 0.625 and 3.125 μg/mL). Tests were conducted in triplicate and reported as average ± standard deviation.

2.7. Preparation and Characterization of Hydrogels Based on Schiff-Base Linkages. *2.7.1. Hydrogel Preparation.* Hydrogels based on Schiff-base linkages were prepared at different polymer concentrations (i.e., 15 and 20% w/v) by simply mixing SHE3350 and AHE1500 aqueous solutions at RT through two polypropylene (PP) syringes (LLG International, Meckenheim, Germany) with a luer-lock connection. In detail, each PEU was solubilized with an aliquot of double-distilled water (i.e., ddH_2O) equal to half the total volume required to prepare a hydrogel at a fixed overall polymer concentration. Then, the two PEU solutions were mixed by slowly sliding them through the luer-lock connector; lastly, the resulting solution was transferred in a Bijou sample container (17 mm diameter, 7 mL, Carlo Erba Reagents, Milan, Italy) and vortexed (1500 rpm) for 1 min. Hydrogels were referred to by the acronym SHE3350−AHE1500_X%, where X defines the overall polymer concentration.

2.7.2. Evaluation of Hydrogel Gelation Time in Physiological-like Conditions. A preliminary evaluation of formulation gelation potential was conducted on SHE3350−AHE1500_20% hydrogels. In detail, hydrogel gelation was studied in physiological-like conditions by incubating the formulations at 37 °C (Memmert IF75, Schwabach, Germany), followed by vial inversion and visual inspection at different time steps (i.e., 15, 30, 45, 60 min, 2, 4, 6, 8, 10, 12, 24 h). The sol-to-gel transition was defined as the absence of flow along the vial walls within 30 s of inversion. The gelation time of formulations with different $-NH_2/-CHO$ molar ratios (ranging between 3:1 and 1:3) was investigated, and the hydrogels were coded as SHE3350−AHE1500_20% Y, where Y defines the $-NH_2/-CHO$ molar ratio, as summarized in Table S1 in the Supporting Information.

2.7.3. Assessment of Imine Bond Formation by ATR-FTIR, Proton, and Carbon-13 Solid-State Nuclear Magnetic Resonance (^{1}H and ^{13}C ssNMR) Spectroscopies. In order to chemically investigate the hydrogel formation driven by Schiff-base bonds, ATR-FTIR, proton, and carbon-13 solid-state nuclear magnetic resonance (^{1}H and ^{13}C ssNMR) spectroscopies were conducted. SHE3350−AHE1500_20% gel was obtained according to the protocol described above. A control sample (SHE3350−AHE1500_20% CTRL) was also prepared following the same method, but the PEU solution resulting from the mixing procedure was rapidly frozen to hinder the Schiff-base bond formation. Samples were freeze-dried (Martin Christ Alpha 2−4 LSC instrument, Germany), and ATR-FTIR spectroscopy was performed according to the previously described protocol. ^{1}H and ^{13}C ssNMR spectroscopic analyses were conducted using a wide bore 11.75 T magnet and a Bruker Avance III spectrometer (Biospin AG, Fällanden, Switzerland) with ^{1}H and ^{13}C operational frequencies of 500.13 and 125.77 MHz, respectively. A 4 mm triple resonance probe, in double resonance mode, with magic angle spinning (MAS), was employed in all experiments, and spectra were accumulated at 298 K. To perform the analysis, 70−80 mg of material were packed on a 4 mm zirconia rotor equipped with a kel-F cap. ^{1}H ssNMR spectra were acquired with a single pulse experiment with a sample spinning rate of 15 kHz. ^{13}C ssNMR spectra were obtained by using the ^{13}C CP-MAS technique with a sample spinning speed of 10 kHz and a CP contact time of 6 ms. All of the chemical shifts are reported on a delta scale and referenced to TMS to 0 ppm. The registered spectra were elaborated using MNova software (Mestrelab Research, S.L, Spain).

2.7.4. Rheological Characterization. Hydrogels based on Schiff-base linkages were rheologically characterized by using a stress-controlled rheometer (MCR302, Anton Paar GmbH, Graz, Austria) equipped with a Peltier system for temperature control and a 15 mm parallel plate configuration. The SHE3350−AHE1500_X% hydrogel was loaded on the rheometer lower plate previously equilibrated at 25 °C. For all of the characterizations, the normal force was set at 0 N. A strain sweep test was performed at 37 °C and a 1 Hz angular frequency from 0.01 to 1200% strain. To evaluate the potential self-healing ability of the gels, samples were again subjected to the same analysis after 30 min of quiescence at 37 °C. Frequency sweep test (frequency range 0.1−100 rad/s) was performed at 0.5% strain at different temperatures (i.e., 25 and 37 °C).

2.7.5. Stability Tests in Physiological-like Conditions. Gel stability in aqueous medium was evaluated by incubation (Memmert IF75, Schwabach, Germany) of the samples in contact with a physiological-like aqueous environment at 37 °C. In detail, 0.5 mL of SHE3350−AHE1500_X% gels were prepared according to the previously described method. Hydrogels were weighted (W_{gel_i}) and equilibrated at 37 °C for 30 min. Subsequently, 1 mL of phosphate-buffered saline (i.e., phosphate-buffered saline (PBS) at pH 7.4, 37 °C) was added to each sample. At predefined time steps (i.e., 7 h, 24 h, 3, 6, 8, 10, 13, 15, 17, 20, 22, 24, 27 days), the residual PBS was removed, the gels were weighted (W_{gel_X}, where X refers to the time step), and put in contact with fresh PBS again. Lastly (i.e., after incubation in contact with PBS for 27 days), samples were freeze-dried and weighted ($W_{dried\ gel\_f}$). Control samples (i.e., SHE3350−AHE1500_X% not incubated in contact with PBS) were also freeze-dried and weighted ($W_{dried\ gel\_i}$). Absorption ability and hydrogel dissolution were estimated according to eqs 1 and 2, respectively

$$\text{wet weight change (\%)} = \frac{W_{gel\_x} - W_{gel\_i}}{W_{gel\_i}} \times 100 \quad (1)$$

$$\text{dry weight change (\%)} = \frac{W_{dried\ gel\_i} - W_{dried\ gel\_f}}{W_{dried\ gel\_i}} \times 100 \quad (2)$$

https://doi.org/10.1021/acsomega.4c03157
ACS Omega 2024, 9, 45774−45788

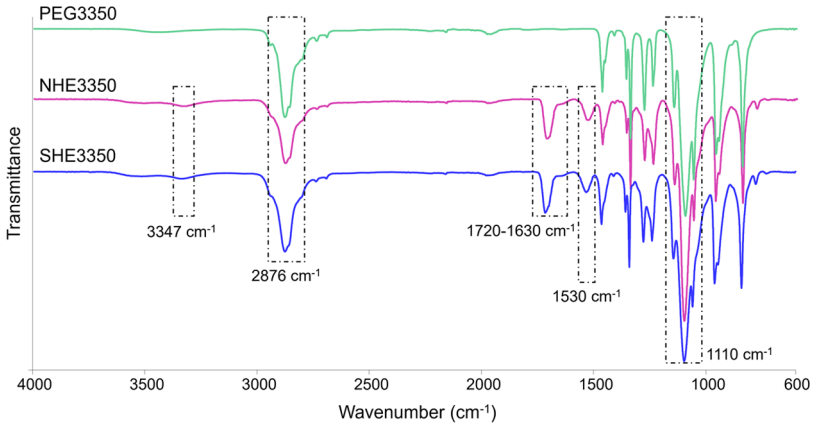

Figure 1. ATR-FTIR spectra of PEG3350 (green line), NHE3350 (pink line), and SHE3350 (blue line). The appearance of new absorption bands at 3347, 1720−1630, and 1530 cm^{-1} proved the successful PEU synthesis and the preservation of its bulk nature after deprotection.

The analyses were conducted in triplicate, and data are reported as average ± standard deviation.

2.7.6. Hydrogel pH Sensitivity in Contact with Alkaline or Acid Buffers. To study gel ability to respond to the acid or alkaline pH of the surrounding environment, stability tests were conducted by incubating the gels at 37 °C (Memmert IF75, Schwabach, Germany) in contact with phosphate buffer solutions at pH 5 and pH 9. Analyses were conducted according to the method described above, and SHE3350−AHE1500_*X*% absorption ability and dissolution in contact with buffers at different pH values were estimated using eqs 1 and 2. The analyses were conducted in triplicate, and data are reported as average ± standard deviation.

2.7.7. Permeability and Release Study of Fluorescein Isothiocyanate Dextran (FD4). Gel permeability to biomolecules and nutrients was qualitatively evaluated by selecting fluorescein isothiocyanate dextran (FD4, M_w 4000 Da, Sigma-Aldrich, Milano, Italy) as a model molecule. Briefly, 1 mL of SHE3350−AHE1500_20% gel was prepared according to the previously described method and incubated at 37 °C (Memmert IF75, Schwabach, Germany) in contact with an FD4 aqueous solution (2 mg/mL, 2:1 v/v with respect to gel volume). At predefined time steps (i.e., 3.5, 7, 12, 24, 36 h), the sample was visually inspected to assess the progressive FD4 uptake. Conversely, to study the FD4 release profile triggered by the pH of the surrounding environment, SHE3350−AHE1500_20% gels were prepared in an FD4 aqueous solution (2 mg/mL), equilibrated at 37 °C for 30 min, and incubated in contact with phosphate buffers at pH 5, 7.4, and 9. The releasing medium was collected at predefined time steps (i.e., 3.5, 7, 24 h, 3, 6, 8, 10, 13, 15, 17 days), and samples were added with fresh buffers. The amount of FD4 released was quantified by measuring the absorbance at 490 nm (PerkinElmer Victor X3) and by referring to a calibration curve based on FD4 solutions prepared in the investigated releasing media (i.e., phosphate buffers at pH 5, 7.4, and 9) at different concentrations ranging between 0.025 and 1 mg/mL. The analyses were conducted in triplicate, and data are reported as average ± standard deviation.

2.7.8. Evaluation of Hydrogel Self-Healing Ability. To qualitatively determine the self-healing ability of the developed hydrogels, two SHE3350−AHE1500_20% gels were prepared according to the previously described protocol. One of them was prepared using a colored aqueous solution (i.e., ddH_2O added with Toluidine Blue O, Sigma-Aldrich, Milano, Italy), thus resulting in a light blue gel disc. Each hydrogel disc was then cut into two parts. The resulting pieces of different colors were connected on the fresh-cut surfaces, ensuring intimate contact to allow the gel to self-heal into an integral sample without any external intervention. To verify the hydrogel integrity, samples were stretched repeatedly.

2.7.9. Evaluation of Hydrogel Injectability. The SHE3350−AHE1500_20% system was prepared according to the method described above and marked with a dye molecule (i.e., Toluidine Blue O). After mixing SHE3350 and AHE1500 solutions, the hydrogel was extruded through a 21-gauge (21G, 0.5 mm inner diameter) needle at different time intervals (i.e., 10−15, 20−30, and 40−50 min) in order to identify the optimal "injectability window", given by the simultaneous fulfillment of three fixed criteria: (i) simple injection with one hand; (ii) injection in an intermediate sol-to-gel state to avoid clogging phenomena; and (iii) gelation within 10−15 min after injection. In order to consider person variability, injectability was tested by two different potential users.

2.8. Statistical Analysis. Statistical analysis was performed using GraphPad Prism 9 for Windows 10 (GraphPad Software, LA Jolla, CA, United States; www.graphpad.com). Two-way analysis of variance (ANOVA) coupled with Bonferroni's multiple comparison test was conducted to compare results. Statistical differences were assessed according to Boffito et al.[24]

3. RESULTS AND DISCUSSION

3.1. Chemical Characterization of NHE3350 and SHE3350 Poly(ether urethane)s. *3.1.1. ATR-FTIR Spectroscopic and Size Exclusion Chromatographic (SEC) Analyses.* ATR-FTIR spectroscopic and SEC analyses were conducted to prove the successful synthesis of both NHE3350 and SHE3350. Figure 1 reports the ATR-FTIR spectra of NHE3350, SHE3350, and PEG3350 as a reference. New absorption bands, generated by the newly formed urethane bonds, were identified in PEU spectra at 3347 and 1720−1630 cm^{-1} due to N−H and C═O stretching vibrations, respectively. Furthermore, the signal at 1530 cm^{-1} was produced by the concurrent N−H bending and C−N stretching. In addition, PEU spectra showed the characteristic absorption peaks of PEG3350 (i.e., $-CH_2$ stretching vibration at 2876 cm^{-1} and C−O−C stretching vibration at 1110 cm^{-1}), thus confirming its inclusion in the PEU chains. The number-average molecular weight ($\overline{M_n}$) and polydispersity index (D) of the synthesized PEUs were *ca.* 24,000 Da and 1.7,

https://doi.org/10.1021/acsomega.4c03157
ACS Omega 2024, 9, 45774−45788

respectively, with no significant differences between three different NHE3350 batches (the typical SEC analysis error has been reported to be in the order of 10%).[33] Moreover, the absence of differences between NHE3350 and SHE3350 in terms of both ATR-FTIR spectra and molecular weight distribution profiles (Figure S1) proved the preservation of the bulk nature of the PEU after the deprotection treatment conducted in acidic conditions for the N-Boc group cleavage.

3.1.2. Proton Nuclear Magnetic Resonance (^{1}H NMR) Spectroscopic Analysis and Quantification of Primary Amines in SHE3350. ^{1}H NMR spectroscopy was performed on NHE3350, SHE3350, and N-Boc serinol to further assess the success of both the synthesis and deprotection processes. The detailed signal assignment to the corresponding protons in the NHE3350 spectrum has been reported in the Supporting Information file (Figure S2), showing chemical shifts ascribed to the chemical structure of the poly(ether urethane) chains. The typical signal of PEG protons appeared between 3.40−3.80 and 4.1 ppm, while the peaks at 1.26, 1.42, and 3.04 ppm belonged to the methylene protons of the diisocyanate-deriving block. Instead, the N-Boc serinol block showed two signals at 3.48−3.59 ppm, partially overlapped to PEG proton resonances, and a single sharp peak at 1.36 ppm due to the methyl protons of the N-Boc protecting groups. This latter peak completely disappeared in the SHE3350 spectrum, as evidenced in Figure 2, thus indicating the successful N-Boc

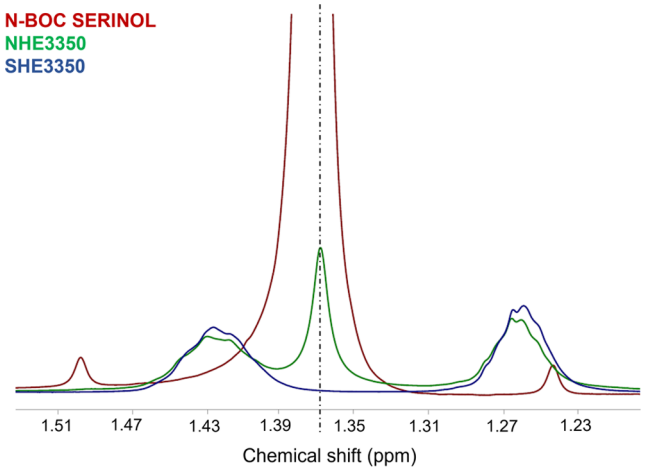

Figure 2. ^{1}H NMR spectra of NHE3350 (green line), SHE3350 (blue line), and N-Boc serinol (red line) in the 1.5−1.2 ppm chemical shift range. The dashed line highlights the peak at 1.36 ppm ascribed to the hydrogens involved in the Boc group.

cleavage and consequently the exposure of 100% of primary amino groups. The signal at 1.36 ppm was also used to indirectly quantify the amount of functionalities exposed along the polymeric chains of three different PEU batches. By referring to the N-Boc serinol spectrum (integration values reported in Figure S3), the number of Boc groups and thus $-NH_2$ units (100% deprotection yield) per gram of polymer was quantified to be $1.96 \times 10^{20} \pm 7.9 \times 10^{18}$. Furthermore, by combining this quantification with SEC results (i.e., $\overline{M}_n$ of *ca.* 24,000 Da), it was possible to establish that each PEU chain contained around six $-NH_2$ units.

The primary amino groups exposed along the SHE3350 polymer backbone were also quantified through the Orange II Sodium Salt colorimetric assay. As shown in Figure 3A, both NHE3350 and SHE3350 samples assumed an orange color after the colorimetric assay. For NHE3350, the orange color was due to the partial Orange molecule adsorption by polymer chains. Conversely, the electrostatic interaction between dye molecules and the exposed primary amino groups (at a 1:1 ratio) resulted in SHE3350 samples stained dark orange. The observed color diversity resulted in significantly different absorbance profiles measured for NHE3350 and SHE3350 samples within 700 and 300 nm, respectively, the dye absorbance peak being positioned at 485 nm (Figure 3B). Moreover, by referring to a calibration curve based on Orange II sodium salt standards, the amount of $-NH_2$ per gram of SHE3350 was measured to be $1.27 \times 10^{20} \pm 2.4 \times 10^{18}$, in agreement with the quantification based on ^{1}H NMR spectra, as summarized in Table 1.

3.2. Chemical Characterization of AHE1500 Poly(ether urethane). *3.2.1. ATR-FTIR Spectroscopic and SEC Analyses.* ATR-FTIR spectroscopic and SEC analyses were conducted to prove the successful synthesis of AHE1500 poly(ether urethane). Figure 4 reports the ATR-FTIR spectra of AHE1500, BA, and PEG1500 as references. The AHE1500 spectrum showed the typical absorption peaks of newly formed urethane bonds (i.e., N−H stretching at 3347 cm^{-1}, C═O stretching at 1720 cm^{-1}, concurrent C−N stretching, and N−H bending at 1530 cm^{-1}), thus confirming its successful synthesis. Moreover, the PEU ATR-FTIR spectrum showed characteristic absorption bands of BA at 1680−1580 cm^{-1} ascribed to the C═C stretching vibration in the aromatic ring. PEG typical bands were also present at 2876 and 1110 cm^{-1} due to $-CH_2$ and C−O−C stretching vibrations, respectively. The number-average molecular weight ($\overline{M}_n$) and polydispersity index (D) of the synthesized PEU were measured to be *ca.* 4000 Da and 1.5, respectively, with no significant differences between three different AHE1500 batches.[22] The molecular weight distribution profiles of three AHE1500 batches have been reported in the Supporting Information file (Figure S4).

3.2.2. ^{1}H NMR Spectroscopic Analysis and Aldehyde Group Quantification. ^{1}H NMR spectroscopy was performed on AHE1500 and BA samples to further characterize the synthesized aldehyde-terminated PEU. As reported in Figures 5 and S5, the AHE1500 spectrum showed the characteristic chemical shifts of the newly formed urethane bonds (at 7.1 ppm, the signal due to the proton of urethane linkages) and PEG-, HDI-, and BA-deriving blocks, thus further proving the success of AHE1500 synthesis. In Figure 5, the appearance in AHE1500 spectrum of peaks at 6.9−8 and 9.75−10 ppm intervals was ascribed to the protons involved in the aromatic ring and to the proton bound to the carbonyl carbon of benzaldehyde groups, respectively. Nevertheless, the appearance of multiple signals in each highlighted region suggested the concurrent existence of two different species of benzaldehyde, polymer-bound (at 9.97, 7.9, and 7.33 ppm) and unbound (at 9.8, 7.75, and 6.9 ppm) BAs, respectively. The presence of free BA as a residual monomer after the PEU synthesis process was in accordance with the ^{1}H NMR results reported by Rahmani et al., who synthesized with a similar method a poly(ether urethane) starting from poly(ethylene glycol) ($\overline{M}_n$ 2000 Da), 1,6-hexamethylene diisocyanate (HDI), and para-hydroxybenzaldehyde and using a catalytic amount of dibutyltin dilaurate as a catalyst.[32]

By exploiting the characteristic absorbance of the BA aromatic ring at around 285 nm, the overall number of

https://doi.org/10.1021/acsomega.4c03157
ACS Omega 2024, 9, 45774−45788

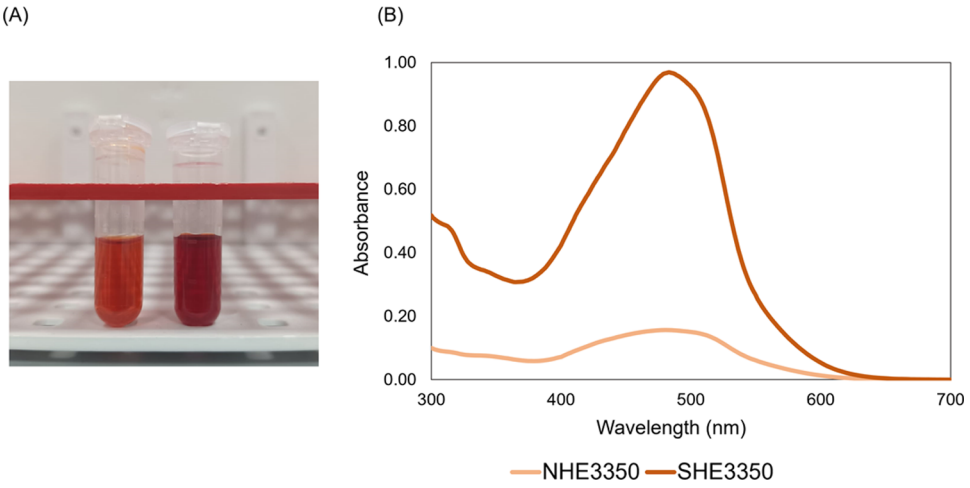

Figure 3. (A) Orange II sodium salt colorimetric assay performed on NHE3350 (light orange marked control sample, on the left) and SHE3350 (dark orange marked deprotected sample, on the right) samples. (B) UV−vis absorbance profiles registered for NHE3350 (light orange line, absorbance at 480 nm due to the adsorbed dye molecules) and SHE3350 (dark orange line, absorbance at 483 nm produced by dye molecules grafted to $-NH_2$ groups and adsorbed to the polymeric chains) samples.

Table 1. Units of $-NH_2$ Functionalities per g of SHE3350 Calculated by UV−Vis and ^{1}H NMR Spectroscopic Analyses

sample	units of $-NH_2$/g of SHE3350 measured from UV−vis	units of $-NH_2$/g of SHE3350 measured from ^{1}H NMR
SHE3350	$1.27 \times 10^{20} \pm 2.4 \times 10^{18}$	$1.96 \times 10^{20} \pm 7.9 \times 10^{18}$

−CHO functionalities in AHE1500 was calculated through UV−vis spectroscopic analyses. By referring to a calibration curve based on BA standards, the amount of −CHO per gram of polymer was measured to be $3.06 \times 10^{20} \pm 1.89 \times 10^{19}$, with no significant differences between three different PEU batches.

3.3. Characterization of Hydrogels Based on Schiff-Base Linkages. *3.3.1. Hydrogel Gelation Time in Physiological-like Conditions.* The gelation kinetics of SHE3350−AHE1500_20% formulations differing for their primary amine/aldehyde molar ratio was studied in physiological-like conditions (i.e., 37 °C) through the tube inverting test. To this aim, the hydrogels were first prepared by mixing SHE3350 and AHE1500 aqueous solutions through two syringes with a luer-lock connection (Figures 6 and S6A). Then, the vials were incubated at 37 °C and inverted at predefined time points to assess the occurrence of gelation, as shown in Figure S6B. The hydrogel resulted from the chemical reaction between the SHE3350 and AHE1500 PEUs. In particular, the condensation reaction between the $-NH_2$ and −CHO groups exposed along the polymer chains led to the formation of imine bonds (−C═N).[34]

As summarized in Table 2, all of the tested formulations underwent gelation. Several studies reported in the literature have shown that an increment in the amount of aldehyde functionalities results in a modulation of hydrogel gelation time, which decreases accordingly.[35,36] Nevertheless, in this work, a different trend was observed, probably ascribable to the presence in the AHE1500 counterpart of two different species of benzaldehyde, free and polymer-bound BAs. Indeed, we observed that an increase in −CHO groups delayed the

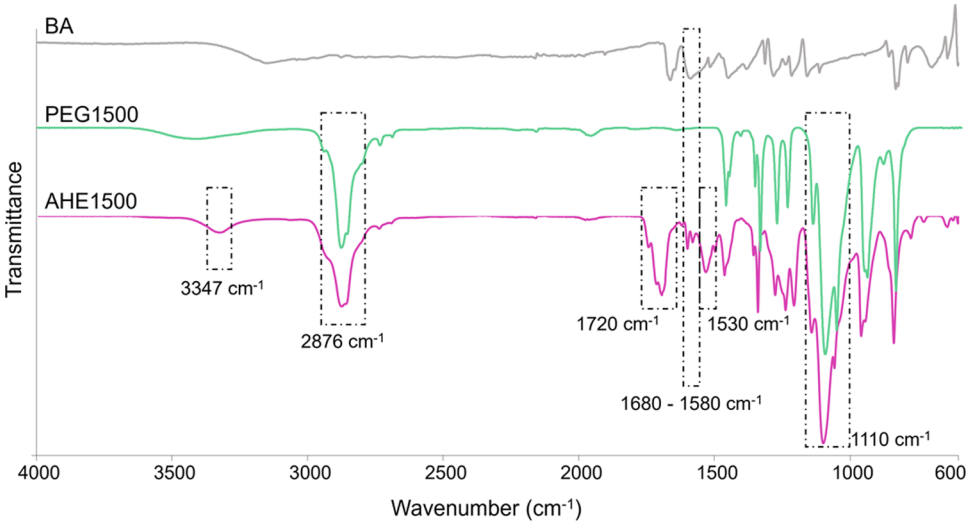

Figure 4. ATR-FTIR spectra of BA (gray line), PEG1500 (green line), and AHE1500 (pink line). The presence of new absorption bands at 3347, 1720, and 1530 cm^{-1} proved the successful PEU synthesis. BA and PEG1500 typical bands were also identified in the AHE1500 ATR-FTIR spectrum at 2876, 1680−1580, and 1110 cm^{-1}.

https://doi.org/10.1021/acsomega.4c03157
ACS Omega 2024, 9, 45774−45788

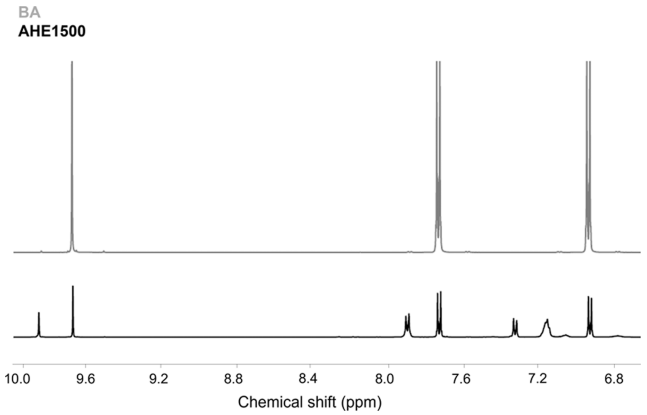

Figure 5. ^{1}H NMR spectra of AHE1500 (black line) and BA (gray line) in the 10 and 6.8 ppm chemical shift ranges. The 9.75−10 and 6.9−8 ppm intervals highlight the peaks ascribed to the hydrogens involved in the benzaldehyde group of both bound and unbound BA molecules.

gelation process (e.g., 24 h and 45 min were needed for the gelation of SHE3350−AHE1500_20% 1:3 and SHE3350−AHE1500_20% 3:1, respectively). This was probably due to the presence in the AHE1500 counterpart of free benzaldehyde molecules, which given their low molecular weight had higher coupling kinetics with the amino groups of SHE3350, compared to the AHE1500 chains. As a result, at the early stage of gel formation, unreacted AHE1500 chains were present in the mixture and a relevant amount of amino groups was capped with BA molecules (Figure S7A). At the second stage, the amino groups still available to form other Schiff-base linkages interacted with the AHE1500-bound benzaldehyde moieties, finally leading to gel network formation and the absence of flow along the vial walls upon tube inversion. Conversely, by enhancing the amino group content and accordingly the SHE3350 polymer concentration in the mixture, the gelation time progressively decreased up to 45 min at an $-NH_2/-CHO$ molar ratio of 3:1 due to the presence of a sufficient number of primary amines to achieve the cross-linking of the polymer chains promoted by AHE1500 (Figure S7B). According to this result, the hydrogels were prepared with an $-NH_2/-CHO$ molar ratio equal to 3:1 and hereafter simply called SHE3350−AHE1500_*X*%, where *X* indicates the overall polymer concentration.

Table 2. Gelation Time of SHE3350−AHE1500_20% Formulations (0.5 mL), Ranging for Their $-NH_2/-CHO$ Molar Ratio between 3:1 and 1:3

sample	$-NH_2$:−CHO molar ratio	gelation time
SHE3350−AHE1500_20% 3:1	3:1	45 min
SHE3350−AHE1500_20% 2:1	2:1	1 h
SHE3350−AHE1500_20% 1:1	1:1	2 h
SHE3350−AHE1500_20% 1:2	1:2	10 h
SHE3350−AHE1500_20% 1:3	1:3	24 h

3.3.2. ATR-FTIR, Carbon-13, and Proton Solid-State Nuclear Magnetic Resonance (^{13}C and ^{1}H ssNMR) Spectroscopic Analyses. To confirm that the developed formulations belonged to the chemically cross-linked hydrogel category and that the sol-to-gel transition was driven by the formation of covalent bonds between amino and aldehyde functionalities, hydrogels were subjected to further chemical characterizations to assess the presence of Schiff-base linkages (i.e., imine bonds C═N). As reported in Figure S8 in the Supporting Information file, the freeze-dried SHE3350−AHE1500_20% ATR-FTIR spectrum showed a shoulder-type absorption peak at 1690−1640 cm^{-1} that was absent in the control sample (i.e., the simple SHE3350/AHE1500 mixture). This absorption band can be ascribed to the C═N stretching vibration,[37] thus demonstrating the presence of the dynamic covalent bond in the hydrogel network. However, as the region of interest corresponded to the typical absorption band ascribed to the urethane bonds of the polymer chains, a clear demonstration of the imine bond formation could not be provided through ATR-FTIR spectroscopy.

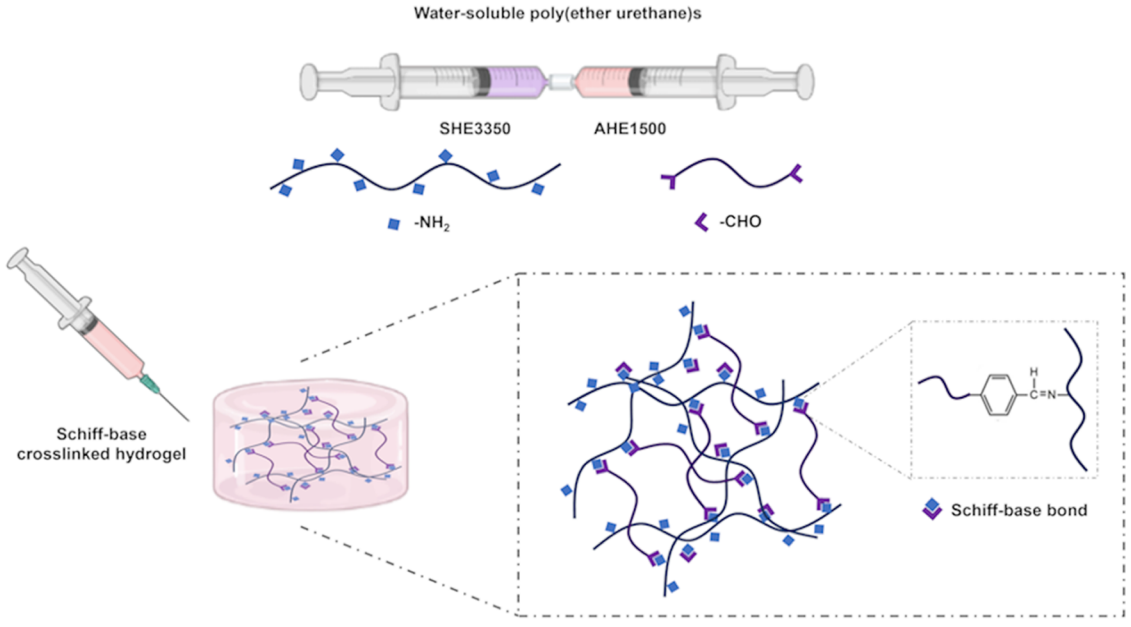

Figure 6. Schematic illustration of injectable hydrogel preparation by simply mixing polymer aqueous solutions resulting in hydrogel network formation through Schiff-base bonds.

https://doi.org/10.1021/acsomega.4c03157
ACS Omega 2024, 9, 45774−45788

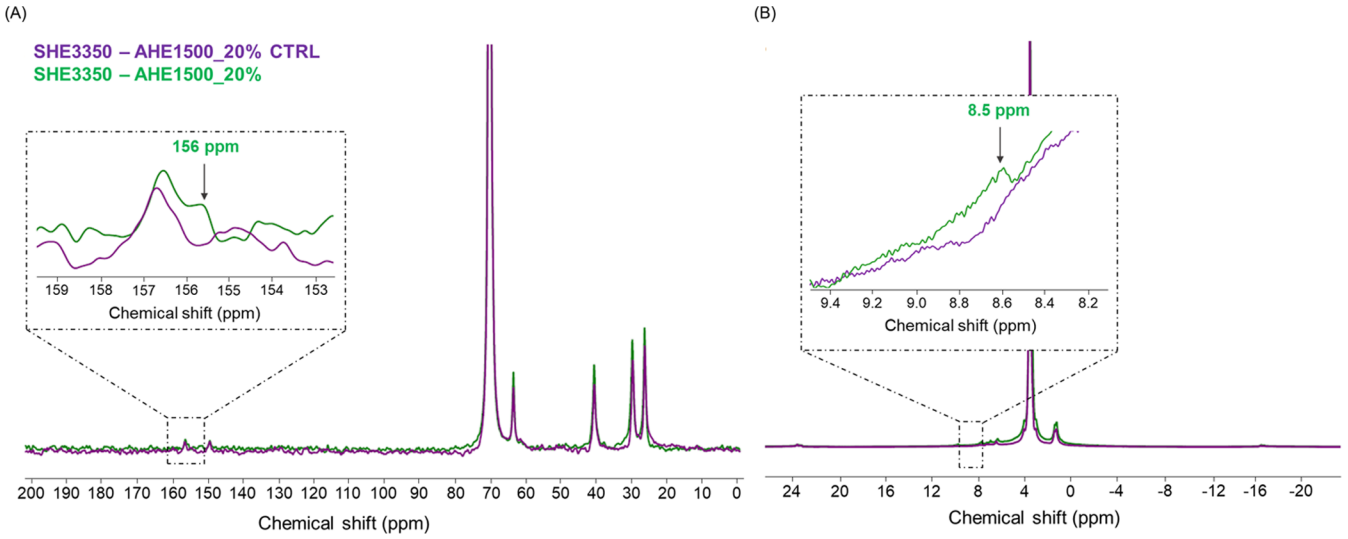

Figure 7. ssNMR spectra of SHE3350−AHE1500_20% mixture (violet line) and hydrogel (green line): (A) the ^{13}C ssNMR spectral magnification in the 153−159 ppm range highlights the appearance of a new peak at 156 ppm that can be ascribed to the carbon double-bonded to nitrogen in Schiff-base linkages; (B) the ^{1}H ssNMR spectral magnification points out the signal at 8.5 ppm ascribed to the imine proton.

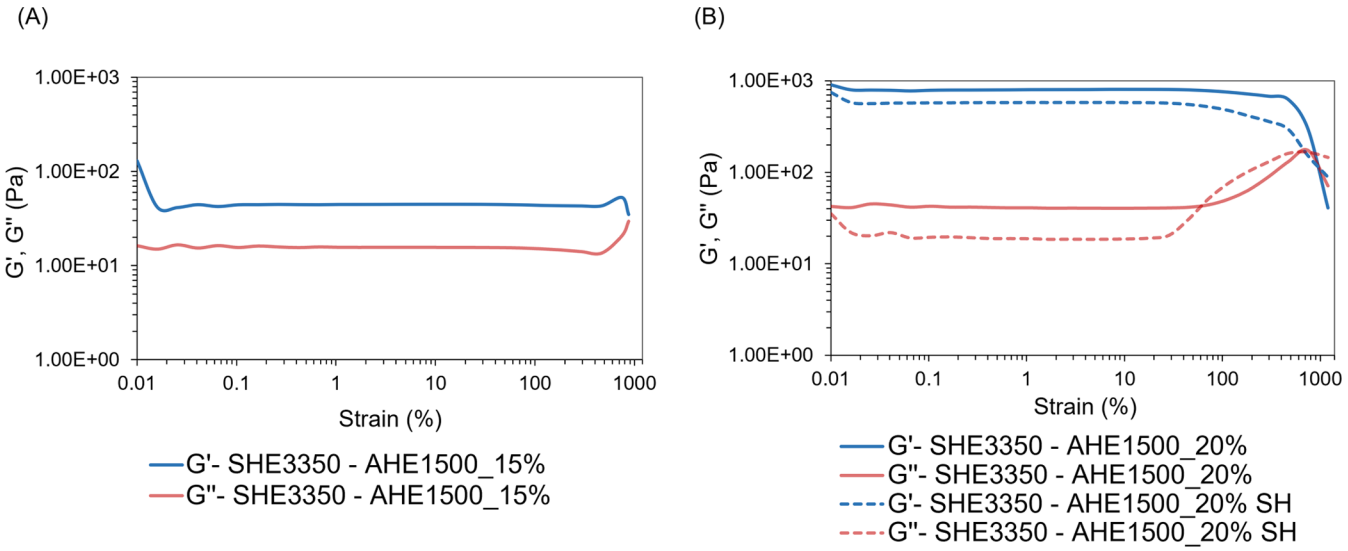

Figure 8. Strain sweep test at 37 °C. Trends of elastic modulus G' (blue line) and viscous modulus G'' (red line) as a function of applied deformation (ranging between 0.01 and 1200% strain) for (A) SHE3350−AHE1500_15% and (B) SHE3350−AHE1500_20% before (continuous lines) and after self-healing for 30 min at 37 °C (acronym SHE3350−AHE1500_20% SH, dashed lines).

The formation of Schiff-base linkages was also investigated by solid-state ^{13}C and ^{1}H NMR spectroscopic analyses. To the best of our knowledge, this is the first time that the ssNMR technique was applied to assess the actual formation of chemical hydrogels based on Schiff-base linkages. Figure 7 displays the SHE3350−AHE1500_20% gel spectrum compared to the PEU mixture as a control. The magnifications evidence the appearance of new signals at 156 and 8.5 ppm in the SHE3350−AHE1500_20% gel spectra that can ascribed to the carbon double-bonded to nitrogen and imine proton in the Schiff-base linkage, respectively.[38,39]

3.3.3. Rheological Characterization of Hydrogels. Rheological characterization was performed on SHE3350−AHE1500 gels with 15 and 20% w/v polymer concentration. Strain sweep tests were conducted to characterize hydrogel behavior in response to applied deformation (γ) (Figure 8), thus identifying the region of viscoelasticity (LVE), within which the samples displayed constant elastic (G') and viscous (G'') moduli. Both the analyzed gels showed a broad LVE region: for SHE3350−AHE1500_20% and SHE3350−AHE1500_15%, the LVE limit was measured to be 120 and 500%, respectively. In addition, for both formulations, G' was greater than G'' (i.e., $G' > G''$) within the LVE, thus proving that the samples were in the gel phase at the tested temperature (i.e., 37 °C). Furthermore, SHE3350−AHE1500_20% showed enhanced mechanical properties compared to SHE3350−AHE1500_15% (i.e., G'-SHE3350−AHE1500_20% higher than G'- SHE3350−AHE1500_15%, 800 Pa *vs* 45 Pa at 1% applied deformation), probably due to the higher cross-linking density of gels at increased polymer concentration. The gel network of SHE3350−AHE1500_20% underwent mechanical failure at high values of applied strain (*ca.* 800−1000%) when G' started to decrease, while G'' became greater, suggesting the formation of cracks within the

https://doi.org/10.1021/acsomega.4c03157
ACS Omega 2024, 9, 45774−45788

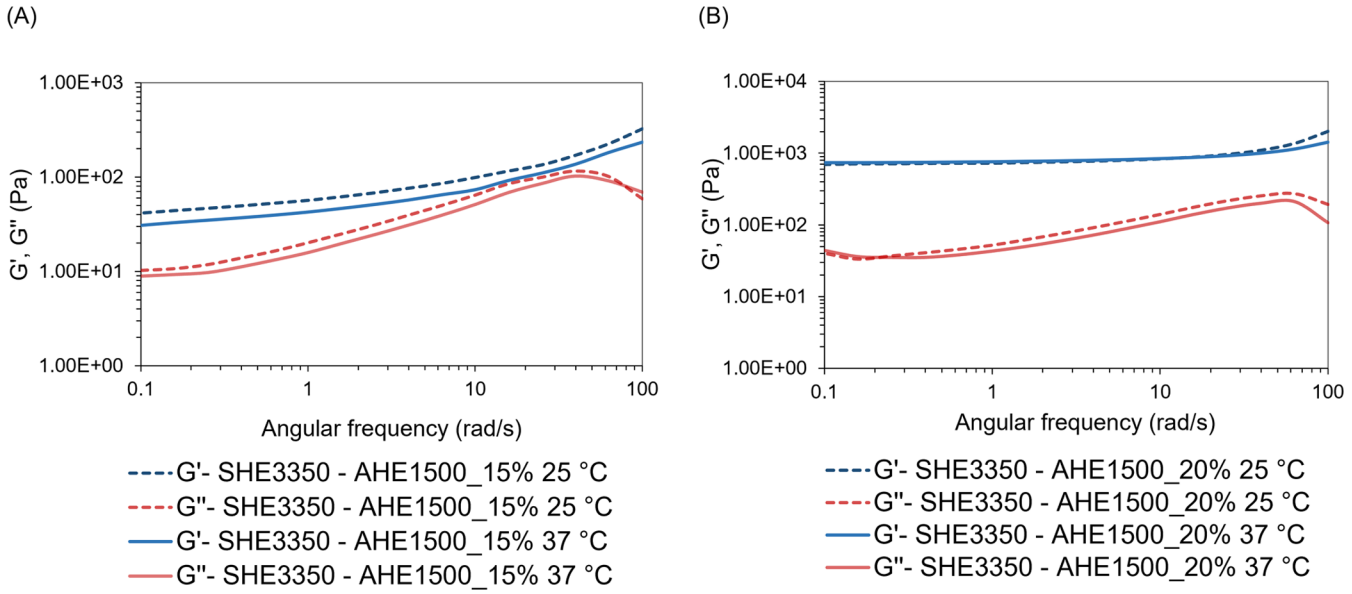

Figure 9. Frequency sweep test at 25 and 37 °C. Trends of elastic modulus G' (blue line) and viscous modulus G'' (red line) as a function of angular frequency for (A) SHE3350−AHE1500_15% and (B) SHE3350−AHE1500_20% at two different temperatures (dashed lines for samples tested at 25 °C, continuous lines for samples tested at 37 °C).

hydrogel network that finally led to the complete sample rupture, with G'' values becoming higher than G'. Conversely, hydrogels at a 15% w/v polymer concentration did not undergo complete rupture even under application of the maximum value of the applied deformation (i.e., 1200%) due to their highly soft nature. To evaluate the potential self-healing ability of SHE3350−AHE1500_20% hydrogels, the strain sweep test was repeated after 30 min of quiescence at 37 °C. Interestingly, a recovery greater than 70% of the starting elastic modulus was observed (800 Pa *vs* 600 at 1% applied deformation); meanwhile, the LVE of the healed samples resulted in less extension due to a decreased ability of healed gels to withstand applied deformations (LVE decrease of around 25%).

The gel state of the hydrogels was also evaluated by frequency sweep tests, conducted at two different temperatures (i.e., 25 and 37 °C). Figure 9 reports the elastic modulus G' and viscous modulus G'' as a function of angular frequency for both the investigated formulations. The samples displayed G' higher than G'' within the analyzed angular frequency range, thus indicating that the formulations were in a gel state. However, G' dependence over the angular frequency for SHE3350−AHE1500_15% suggested that this sample was not a fully developed gel, in accordance with the lower mechanical properties observed by the strain sweep test. Lastly, no differences in G' and G'' trends were recorded by changing the testing temperature, thus proving the absence of thermoresponsiveness.

3.3.4. Stability Tests in Physiological-like Conditions. The stability of the designed hydrogels based on Schiff-base linkages was tested in physiological-like conditions (i.e., in contact with phosphate buffer saline, PBS, at pH 7.4 and 37 °C). SHE3350−AHE1500 gels showed relevant fluid absorption ability and stability over time at both the considered polymer concentrations. As shown in Figure 10, hydrogels increased their wet weight by 70% at 7 h of incubation, with no significant differences between the two tested formulations. Furthermore, the PBS absorption reached a plateau value

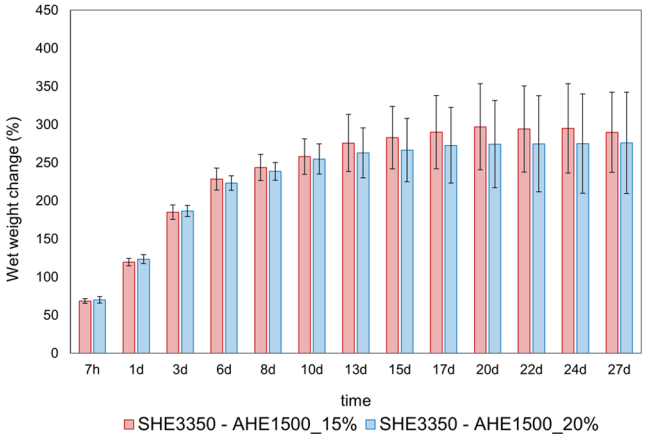

Figure 10. Hydrogel wet weight change (%) as a function of time for SHE3350−AHE1500 gels with 15% w/v (red bars) and 20% w/v (light blue bars) polymer concentration during incubation in contact with PBS. Both the tested formulations showed high buffer absorption ability and stability up to 27 days in contact with phosphate buffer saline (i.e., PBS at pH 7.4).

starting from 13 days of incubation. After 27 days of incubation in contact with PBS, a *ca.* 270% wet weight change was measured for both SHE3350−AHE1500_20% and SHE3350−AHE1500_15%, coupled with a dry weight loss of around 40%. The high absorption ability and stability of the developed gels could be explained by considering their chemical cross-linked nature: the covalent linkages between the polymeric chains allow high buffer absorption without early dissolution. Overall, no significant differences were observed between SHE3350−AHE1500_20% and SHE3350−AHE1500_15% samples within the analyzed time interval.

3.3.5. pH Sensitivity in Contact with Buffers at Acidic or Alkaline pH. It is known that Schiff-base bonds are pH-sensitive under acidic conditions, meaning that the hydrogel stability could be compromised in contact with environments at low pH.[40,41] For this reason, gel absorption ability and

https://doi.org/10.1021/acsomega.4c03157
ACS Omega 2024, 9, 45774−45788

dissolution behavior were investigated at different pH values by incubating SHE3350−AHE1500 gels at 37 °C in phosphate buffers at acidic or alkaline pH (i.e., pH 5 and pH 9, respectively). Figure 11 reports the percentage of the hydrogel

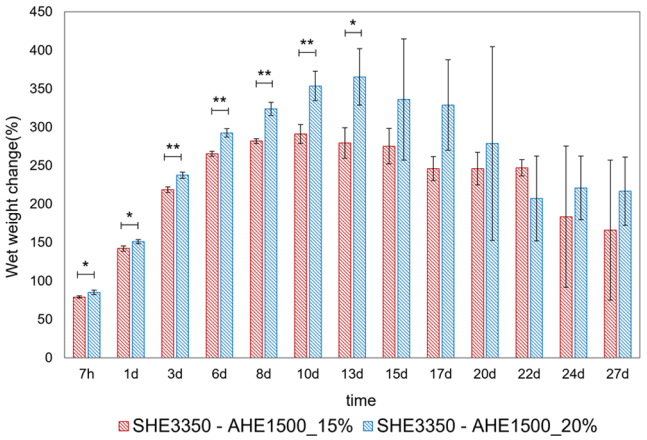

Figure 11. Hydrogel wet weight change (%) as a function of time for SHE3350−AHE1500 gels with 15% w/v (red bars) and 20% w/v (light blue bars) polymer concentration during incubation in contact with a phosphate buffer at pH 5. Under this testing condition, both the tested formulations showed increased buffer absorption ability until dissolution phenomena started to occur (*p < 0.05, **p < 0.01).

wet weight change measured during incubation in contact with a buffer at pH 5. SHE3350−AHE1500 hydrogels displayed enhanced absorption ability at 7 h compared to samples tested in physiological-like conditions (i.e., 80% *vs* 70%), with significant differences between the two tested formulations (p = 0.0325). The maximum buffer absorption was reached at around 10 days for SHE3350−AHE1500_15% (290% increase in wet weight) and at 13 days for SHE3350−AHE1500_20% (wet weight gain of 360%). Thereafter, the gel wet weight started to decrease due to imine bond hydrolysis at low pH. In fact, the reversibility of the Schiff-base bonds in acidic conditions involved the breaking of the linkages between the polymeric chains of the gel network, thus resulting in both increased initial buffer absorption and subsequent dissolution phenomena. This trend was more pronounced for SHE3350−AHE1500_20%, probably due to the higher number of imine bonds forming the gel network compared to SHE3350−AHE1500_15%. After 27 days of incubation in contact with a buffer at pH 5, the dry weight of the samples decreased to 70% irrespective of the hydrogel polymer concentration. Hence, the dry weight change at pH 5 was significantly higher compared to that at pH 7.4 (70% *vs* 40%) as a consequence of sample susceptibility to acidic-pH-triggered hydrolysis of Schiff-base bonds.

Conversely, lower absorption was observed when the gels were incubated in contact with a phosphate buffer at alkaline pH (i.e., pH 9), as reported in Figure 12. At the early stage of incubation, the wet weight of both the gel formulations increased by only 45%, reaching a value of approximately 200% at 27 days, with a reduction of the dry weight of 40%. This behavior could be explained by considering the progressive buffer ion uptake that promoted salting-out phenomena leading to gel shrinkage and thus reduced the percentage of wet weight change compared to samples incubated with PBS.[42] Similarly to sample incubation with PBS, no significant differences were observed between SHE3350−

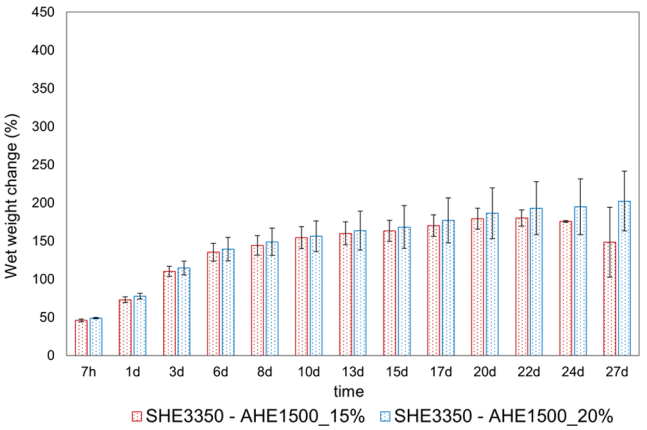

Figure 12. Hydrogel wet weight change (%) as a function of time for SHE3350−AHE1500 gels with 15% w/v (red bars) and 20% w/v (light blue bars) polymer concentration during incubation in contact with a phosphate buffer at pH 9. Under this testing condition, both the tested formulations showed limited buffer absorption ability compared to hydrogels incubated with PBS.

AHE1500_20% and SHE3350−AHE1500_15% samples within the analyzed time interval.

Considering the rheological and stability outcomes, SHE3350−AHE1500_20% was selected as a promising formulation for further investigations.

3.3.6. Study of Permeability and Release Profile of FD4 Model Molecule from SHE3350−AHE1500 Gels. FD4 was selected for both permeability and payload release studies since it represents a model molecule of drugs and biomolecules.[43] As shown in Figure 13, the capability of SHE3350−AHE1500_20% gels to absorb FD4 molecules was qualitatively proved by the appearance of a colored gradient advancing through the sample thickness over time. Overall, the hydrogel possessed high permeability, achieving equilibrium in molecule uptake within 36 h of incubation. Since the developed formulations showed different fluid absorption abilities and stabilities in response to the environmental pH, FD4 was encapsulated at 1 mg/mL concentration within the gels and its release was studied at pH 5, 7.4, and 9 to investigate whether the drug release could be pH-triggered. A schematic illustration of hydrogel drug loading (Figure S9A) and release mechanism in contact with the environment at different pH values (Figure S9B,C) was reported in the Supporting Information file. The trends of FD4 release (Figure 14) were then defined through specifically designed calibration curves based on FD4 standards with different concentrations and prepared in phosphate buffer at pH 5, 7.4, and 9 (Figure S10). A sustained release of up to 17 days was measured from SHE3350−AHE1500_20% gels at the three pH conditions. In physiological-like condition (i.e., at pH 7.4), a controlled release profile was recorded and a complete FD4 release was reached after 2 weeks. Conversely, since the early stage of incubation, FD4 release in contact with an alkaline environment was significantly higher than that at pH 5 or pH 7.4 (i.e., at 24 h of incubation, FD4 concentration in the release medium was measured to be 0.5 ± 0.005, 0.25 ± 0.01, and 0.35 ± 0.01 mg/mL at pH 9, 5, and 7.4, respectively). Then, the FD4 release reached a plateau value at 8 days and almost the total amount of encapsulated molecule was released (i.e., 0.95 ± 0.02 mg/mL at 17 days). This result is in accordance with stability test data measured at pH 9 (Figure 12). Indeed, the hydrogel shrinkage phenomena

https://doi.org/10.1021/acsomega.4c03157
ACS Omega 2024, 9, 45774−45788

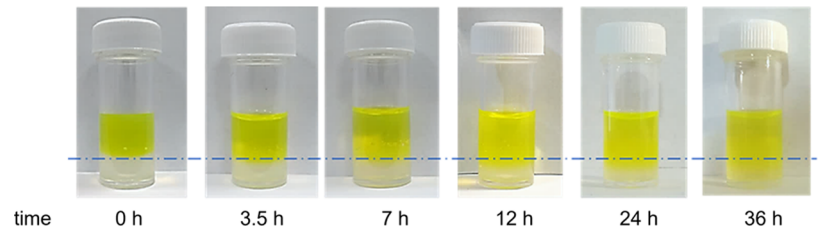

Figure 13. Qualitative evaluation of the SHE3350−AHE1500_20% gel permeability to FD4 as a model molecule. Progressive molecule uptake is evidenced by the appearance of a colored gradient advancing through the sample thickness over time. Equilibrium was achieved within 36 h of incubation.

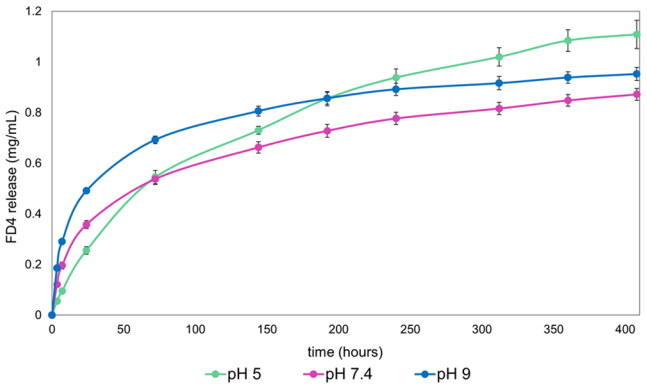

Figure 14. FD4 release profile (1 mg/mL) from 20% w/v concentrated hydrogels in contact with phosphate buffers at pH 5 (green line), pH 7.4 (pink line), and pH 9 (blue line). pH 5 *vs* pH 7.4: ****$p < 0.0001$ at 3.5 h, ***$p < 0.001$ at 7 h, **$p < 0.01$ at 24, 192, 240, 312, 360, and 408 h, *$p < 0.05$ at 144 h, ns ($p > 0.05$) at 72 h. pH 5 *vs* pH 9: **** at 3.5, 7, and 24 h, ** at 72, 144, and 360 h, * at 312 and 408 h, ns at 192 and 240 h. pH 7.4 *vs* pH 9: **** at 3.5 h, *** at 7, 24, and 72 h, ** at 144, 192, 240, 312, and 360 h, * at 408 h.

observed at high pH value could cause enhanced release of the drug molecules.[44] At pH 5, the process of FD4 release was affected by the progressive acidic-pH-triggered imine bond hydrolysis and the consequent hydrogel dissolution (Figure S9C). Nevertheless, at pH 5, no burst release was observed and the amount of released FD4 molecules was lower compared to pH 7.4 and 9 conditions (i.e., at 7 h of incubation, FD4 concentration in the release medium was measured to be 0.09 ± 0.01, 0.19 ± 0.01, and 0.29 ± 0.0005 mg/mL at pH 5, 7.4, and 9, respectively). However, at 72 and 192 h of incubation, significant changes in release kinetics occurred, as from these time points, the FD4 release at pH 5 was always higher than pH 7.4 and pH 9, respectively, reaching a complete release after 13 days of incubation.

3.3.7. Evaluation of Hydrogel Self-Healing Ability. The self-healing ability of gels based on Schiff-base linkages represents one of the major properties of *in situ* drug delivery formulations, since these systems are able to naturally recover their initial structure, thus preserving their integrity. In this work, gel self-healing potential was qualitatively evaluated by placing SHE3350−AHE1500_20% half discs in contact along the cut ends (Figure 15A). The two pieces merged into an integral gel after 20−30 min of intimate contact at RT, as a result of the dynamic nature of imine covalent bonds. To prove the remarkable self-healing properties, the healed hydrogel was repeatedly stretched at both ends and no cracks or ruptures were observed (Figure 15B).

3.3.8. Evaluation of the Hydrogel Injectability. To design a reliable platform for *in situ* drug delivery and tissue engineering

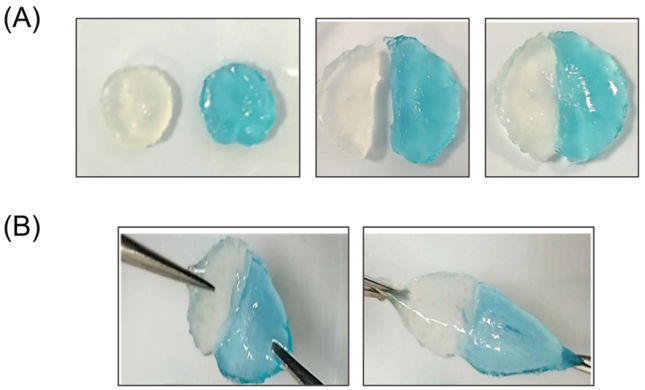

Figure 15. Qualitative evaluation of the hydrogel self-healing ability (A) by cutting two gel discs and ensuring the intimate contact between the pieces and (B) by applying repeatedly mechanical stress, thus proving the remarkable self-healing property.

applications, a standardized injection procedure was defined. The SHE3350−AHE1500_20% hydrogel was injected using a standard 21G needle with a 0.5 mm inner diameter after mixing the SHE3350 and AHE1500 starting solutions through syringes with a luer-lock connection. Then, three different time intervals of injections were investigated, i.e., 10−15, 20−30, and 40−50 min after mixing (Table 3).

Table 3. Identification of the Optimal "Injectability Window"[a]

	CRITERIA		
interval of injection after mixing	injection with one hand	injection in an intermediate sol-to-gel state to avoid clogging phenomena	gelation within 10−15 min after injection
10−15 min	√	√	X
20−30 min	√	√	√
40−50 min	X	X	-

[a] √ and X marks indicate the criterion fulfillment or fail, respectively; the dash stands for an excluded criterion.

As shown in Figure 16A and summarized in Table 3, at 10−15 min after hydrogel formulation mixing, easy injectability with one hand and without clogging phenomena was reported by both potential users that performed the test. However, complete gelation did not occur within 10−15 min after injection, as confirmed by the presence of flow along the vial walls within 30 s of inversion. Conversely, at 40−50 min, the formulation in the syringe appeared in a gel state, thus requiring excessive force to achieve injection and showing needle-clogging phenomena (Figure 16C and Table 3). Hence, 20−30 min was selected as the optimal "injectability window",

https://doi.org/10.1021/acsomega.4c03157
ACS Omega 2024, 9, 45774−45788

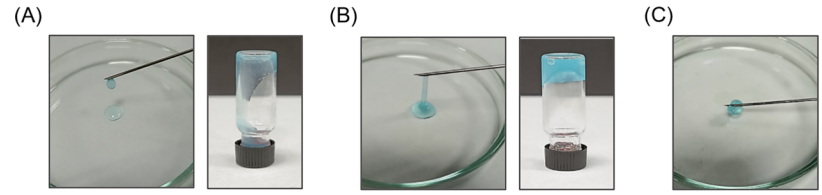

Figure 16. Injection procedure at (A) 10−15 min, (B) 20−30 min, and (C) 40−50 min after hydrogel formulation mixing.

since the three criteria were simultaneously satisfied: the hydrogel formulation was easily injectable in an intermediate sol-to-gel state, and once injected, complete gelation occurred within 10−15 min (Figure 16B and Table 3).

4. CONCLUSIONS

In this work, *in situ*-forming injectable hydrogels with promising features for drug delivery applications were successfully engineered by exploiting the versatility of Schiff-base poly(ether urethane) chemistries. Two water-soluble PEUs (termed SHE3350 and AHE1500) with tuned molecular weight and a significant number of primary amines and aldehydes were synthesized. While SHE3350 did not show any residual byproducts after synthesis, AHE1500 still contained a fraction of unbound BA molecules, suggesting the need for further optimization of the purification phase of this material, e.g., through additional precipitation steps, dialysis against a BA solubilizing solvent (e.g., acetone, alcohol) or chromatographic columns. Despite this concern that is currently under investigation in our group, chemical hydrogels based on Schiff-base linkages were successfully obtained by simply mixing aqueous solutions of SHE3350 and AHE1500 at an optimized $-NH_2/-CHO$ molar ratio and overall polymer concentration. Chemical characterization by ^{13}C and ^{1}H ssNMR spectroscopies confirmed the presence of imine bonds as cross-linking points in the hydrogel network, while rheological tests evidenced the gel state of the formulation, its high resistance to applied strain, and self-healing potential. Furthermore, fluid absorption and dissolution behavior in physiological-like conditions showed high buffer absorption and stability for up to 27 days. When in contact with buffers at acidic or alkaline pH, hydrogels exhibited increased buffer absorption ability followed by early dissolution at pH 5 and shrinkage phenomena induced by the salting-out effect at pH 9. The developed hydrogels proved to be highly permeable to FD4 model molecules, gaining equilibrium in the molecule uptake within 36 h of incubation. We also demonstrated the ability of the designed formulations to release FD4 molecules in a controlled and sustained manner. Moreover, the possibility to differentiate the release kinetics according to the environmental pH makes them versatile drug delivery platforms in tissue engineering applications. Besides proving the injectability of the hydrogels, a standardized procedure for injectability assessment was defined, leading to the definition of the optimal "injectability window" based on the fulfillment of three criteria. Lastly, the developed hydrogels based on Schiff-base linkages displayed a clear self-healing ability after network damage. In conclusion, our results highlight that the hydrogel platform described here is clearly promising for *in situ* drug delivery and tissue engineering applications, thanks to its good stability in physiological-like conditions, pH sensitivity, injectability, and self-healing that enable localized therapy and improve formulation durability upon application. In addition, the developed hydrogels can find application in minimally invasive procedures and whenever a prolonged *in situ* pH-triggered payload delivery is needed. In this regard, toward the progressive translation of the developed hydrogel formulations from the bench to the bedside, molecules with a therapeutic potential (e.g., drugs, growth factors, nucleic acids) need to be selected according to the targeted application and loaded within the hydrogels during preparation. Then, the hydrogels' therapeutic potential will be biologically assessed initially through cytocompatibility tests and then through functional assays evaluating the retained drug functionality upon encapsulation and release. According to a sustainable and ethically compliant approach, these tests will be conducted on increasingly complex biological models, encompassing bi-dimensional cell cultures, three-dimensional *in vitro* bioengineered tissue/organ models, and *in vivo* models. In this regard, *in vivo* studies will also be relevant to investigate the residence time of the developed formulations in their real working scenario and assess potential unexpected side effects of the hydrogel themselves and released molecules (i.e., encapsulated payload and degradation products). According to the selected final application, an additional fine-tuning of the hydrogel residence time would potentially be needed. In this context, the combination of poly(urethane) and Schiff-base chemistries could be exploited to confer highly tunable properties to the developed formulations, including those related to their degradability. For instance, the observed acidic-pH-responsiveness could be tuned by modulating hydrogel composition to achieve a pH-triggered release in acidic environments, which often characterize some pathological milieus (e.g., inflamed tissues or tumors). Furthermore, the inclusion of specific amino acid sequences along the PEU backbone could be exploited to provide the synthesized material with additional sensitivity to enzyme-triggered hydrolysis. Overall, we hypothesize that the system can be *ad hoc*-tuned to meet the specific therapeutic needs of the targeted application, which represents a highly demanding need for the development of functional therapeutic approaches.

■ ASSOCIATED CONTENT

Supporting Information

The Supporting Information is available free of charge at https://pubs.acs.org/doi/10.1021/acsomega.4c03157.

Molecular weight distribution profiles of the synthesized poly(ether urethane)s, ^{1}H NMR spectra of the synthesized poly(ether urethane)s, photographs of hydrogel preparation, schematic illustration of hydrogel formation, ATR-FTIR spectrum of the Schiff-base hydrogel, calibration curve of fluorescein isothiocyanate dextran model molecule, and schematic view of drug loading and release mechanism (PDF)

https://doi.org/10.1021/acsomega.4c03157
ACS Omega 2024, 9, 45774−45788

AUTHOR INFORMATION

Corresponding Authors

Monica Boffito − *Department of Mechanical and Aerospace Engineering, Politecnico di Torino, 10129 Turin, Italy;* orcid.org/0000-0001-7637-2001; Email: monica.boffito@polito.it

Gianluca Ciardelli − *Department of Mechanical and Aerospace Engineering, Politecnico di Torino, 10129 Turin, Italy; Department of Life Sciences, Università di Modena e Reggio Emilia, 41125 Modena, Italy;* orcid.org/0000-0003-0199-1427; Email: gianluca.ciardelli@polito.it

Authors

Roberta Pappalardo − *Department of Mechanical and Aerospace Engineering, Politecnico di Torino, 10129 Turin, Italy; Department of Surgical Sciences, Università degli Studi di Torino, 10126 Turin, Italy*

Claudio Cassino − *Department of Science and Technological Innovation, Università del Piemonte Orientale, 15121 Alessandria, Italy;* orcid.org/0000-0002-7785-2717

Valeria Caccamo − *Department of Mechanical and Aerospace Engineering, Politecnico di Torino, 10129 Turin, Italy*

Valeria Chiono − *Department of Mechanical and Aerospace Engineering, Politecnico di Torino, 10129 Turin, Italy;* orcid.org/0000-0003-2067-7732

Complete contact information is available at: https://pubs.acs.org/10.1021/acsomega.4c03157

Author Contributions

[⊥]R.P. and M.B. contributed equally to this work. The manuscript was written through contributions of all authors. All authors have given approval to the final version of the manuscript. Conceptualization, R.P. and M.B.; methodology, R.P., M.B., and C.C.; validation, R.P. and M.B.; formal analysis, R.P. and C.C.; investigation, R.P., M.B., C.C., and V.C. (V. Caccamo); resources, G.C.; data curation, R.P. and M.B.; writing—original draft preparation, R.P.; writing—review and editing, M.B., C.C., V.C. (V. Caccamo), V.C. (V. Chiono), and G.C.; visualization, R.P.; supervision, G.C. and V.C. (V. Chiono); and funding acquisition, G.C.

Funding

The research leading to these results has received funding from the European Union-NextGenerationEU through the Italian Ministry of University and Research under PNRR-M4C2−I1.3 Project PE00000019 "HEAL ITALIA" to Gianluca Ciardelli CUP E93C22001860006 of Università di Modena e Reggio Emilia. The views and opinions expressed are those of the authors only and do not necessarily reflect those of the European Union or European Commission. Neither the European Union nor the European Commission can be held responsible for them.

Notes

The authors declare no competing financial interest.

ACKNOWLEDGMENTS

The authors acknowledge funding from the European Union-NextGenerationEU through the Italian Ministry of University and Research under PNRR-M4C2.I1.3 Project PE00000019 "HEAL ITALIA".

REFERENCES

(1) Ho, T. C.; Chang, C. C.; Chan, H. P.; Chung, T. W.; Shu, C. W.; Chuang, K. P.; Duh, T. H.; Yang, M. H.; Tyan, Y. C. Hydrogels: Properties and Applications in Biomedicine. *Molecules* **2022**, *27* (9), 1−29.

(2) Yang, J. A.; Yeom, J.; Hwang, B. W.; Hoffman, A. S.; Hahn, S. K. In Situ-Forming Injectable Hydrogels for Regenerative Medicine. *Prog. Polym. Sci.* **2014**, *39* (12), 1973−1986.

(3) Yu, L.; Ding, J. Injectable Hydrogels as Unique Biomedical Materials. *Chem. Soc. Rev.* **2008**, *37* (8), 1473−1481.

(4) Li, Y.; Yang, H. Y.; Lee, D. S. Biodegradable and Injectable Hydrogels in Biomedical Applications. *Biomacromolecules* **2022**, *23* (3), 609−618.

(5) Rizzo, F.; Kehr, N. S. Recent Advances in Injectable Hydrogels for Controlled and Local Drug Delivery. *Adv. Healthcare Mater.* **2021**, *10* (1), 1−26.

(6) Pandya, A. K.; Vora, L. K.; Umeyor, C.; Surve, D.; Patel, A.; Biswas, S.; Patel, K.; Patravale, V. B. Polymeric in Situ Forming Depots for Long-Acting Drug Delivery Systems. *Adv. Drug Delivery Rev.* **2023**, *200*, No. 115003.

(7) Hu, W.; Wang, Z.; Xiao, Y.; Zhang, S.; Wang, J. Advances in Crosslinking Strategies of Biomedical Hydrogels. *Biomater. Sci.* **2019**, *7* (3), 843−855.

(8) Yang, J.; Chen, Y.; Zhao, L.; Zhang, J.; Luo, H. Constructions and Properties of Physically Cross-Linked Hydrogels Based on Natural Polymers. *Polym. Rev.* **2023**, *63* (3), 574−612.

(9) Nam, K.; Watanabe, J.; Ishihara, K. The Characteristics of Spontaneously Forming Physically Cross-Linked Hydrogels Composed of Two Water-Soluble Phospholipid Polymers for Oral Drug Delivery Carrier I: Hydrogel Dissolution and Insulin Release under Neutral PH Condition. *Eur. J. Pharm. Sci.* **2004**, *23* (3), 261−270.

(10) Li, X.; Xiong, Y. Application of "Click" Chemistry in Biomedical Hydrogels. *ACS Omega* **2022**, *7* (42), 36918−36928.

(11) Pérez-Madrigal, M. M.; Shaw, J. E.; Arno, M. C.; Hoyland, J. A.; Richardson, S. M.; Dove, A. P. Robust Alginate/Hyaluronic Acid Thiol-Yne Click-Hydrogel Scaffolds with Superior Mechanical Performance and Stability for Load-Bearing Soft Tissue Engineering. *Biomater. Sci.* **2020**, *8* (1), 405−412.

(12) Mironi-Harpaz, I.; Wang, D. Y.; Venkatraman, S.; Seliktar, D. Photopolymerization of Cell-Encapsulating Hydrogels: Crosslinking Efficiency versus Cytotoxicity. *Acta Biomater.* **2012**, *8* (5), 1838−1848.

(13) Xu, J.; Liu, Y.; Hsu, S. H. Hydrogels Based on Schiff Base Linkages for Biomedical Applications. *Molecules* **2019**, *24* (16), 1−21.

(14) Xin, Y.; Yuan, J. Schiff's Base as a Stimuli-Responsive Linker in Polymer Chemistry. *Polym. Chem.* **2012**, *3* (11), 3045−3055.

(15) Sahajpal, K.; Shekhar, S.; Kumar, A.; Sharma, B.; Meena, M. K.; Bhagi, A. K.; Sharma, S. Dynamic Protein and Polypeptide Hydrogels Based on Schiff Base Co-Assembly for Biomedicine. *J. Mater. Chem. B* **2022**, *10* (17), 3173−3198.

(16) Malik, U. S.; Niazi, M. B. K.; Jahan, Z.; Zafar, M. I.; Vo, D. V. N.; Sher, F. Nano-Structured Dynamic Schiff Base Cues as Robust Self-Healing Polymers for Biomedical and Tissue Engineering Applications: A Review. *Environ. Chem. Lett.* **2022**, *20* (1), 495−517.

(17) Li, S.; Pei, M.; Wan, T.; Yang, H.; Gu, S.; Tao, Y.; Liu, X.; Zhou, Y.; Xu, W.; Xiao, P. Self-Healing Hyaluronic Acid Hydrogels Based on Dynamic Schiff Base Linkages as Biomaterials. *Carbohydr. Polym.* **2020**, *250* (May), No. 116922.

(18) Wei, Z.; Zhao, J.; Chen, Y. M.; Zhang, P.; Zhang, Q. Self-Healing Polysaccharide-Based Hydrogels as Injectable Carriers for Neural Stem Cells. *Sci. Rep.* **2016**, *6*, No. 37841.

(19) Lee, Y.-M.; Lu, Z.-W.; Wu, Y.-C.; Liao, Y.-J.; Kuo, C.-Y. An Injectable, Chitosan-Based Hydrogel Prepared by Schiff Base Reaction for Anti-Bacterial and Sustained Release Applications. *Int. J. Biol. Macromol.* **2024**, *269*, No. 131808.

(20) Shi, J.; Guobao, W.; Chen, H.; Zhong, W.; Qiu, X.; Xing, M. M. Q. Schiff Based Injectable Hydrogel for in Situ PH-Triggered Delivery of Doxorubicin for Breast Tumor Treatment. *Polym. Chem.* **2014**, *5* (21), 6180−6189.

(21) Du, M.; Jin, J.; Zhou, F.; Chen, J.; Jiang, W. Dual Drug-Loaded Hydrogels with PH-Responsive and Antibacterial Activity for Skin Wound Dressing. *Colloids Surf., B* **2023**, *222* (November 2022), No. 113063.
(22) Shahi, S.; Roghani-mamaqani, H.; Talebi, S.; Mardani, H. Chemical Stimuli-Induced Reversible Bond Cleavage in Covalently Crosslinked Hydrogels. *Coord. Chem. Rev.* **2022**, *455*, No. 214368.
(23) Martorana, A.; Lenzuni, M.; Contardi, M.; Palumbo, F. S.; Cataldo, S.; Pettignano, A.; Catania, V.; Schillaci, D.; Summa, M.; Athanassiou, A.; Fiorica, C.; Bertorelli, R.; Pitarresi, G. Schiff Base-Based Hydrogel Embedded with In Situ Generated Silver Nanoparticles Capped by a Hyaluronic Acid-Diethylenetriamine Derivative for Wound Healing Application. *ACS Appl. Mater. Interfaces* **2024**, *16* (16), 20186−20201, DOI: 10.1021/acsami.4c00657.
(24) Boffito, M.; Gioffredi, E.; Chiono, V.; Calzone, S.; Ranzato, E.; Martinotti, S.; Ciardelli, G. Novel Polyurethane-Based Thermosensitive Hydrogels as Drug Release and Tissue Engineering Platforms: Design and in Vitro Characterization. *Polym. Int.* **2016**, *65* (7), 756−769.
(25) Laurano, R.; Boffito, M. Thermosensitive Micellar Hydrogels as Vehicles to Deliver Drugs With Different Wettability. *Front. Bioeng. Biotechnol.* **2020**, *8* (July), No. 708.
(26) Laurano, R.; Boffito, M.; Abrami, M.; Grassi, M.; Zoso, A.; Chiono, V.; Ciardelli, G. Dual Stimuli-Responsive Polyurethane-Based Hydrogels as Smart Drug Delivery Carriers for the Advanced Treatment of Chronic Skin Wounds. *Bioact. Mater.* **2021**, *6* (9), 3013−3024.
(27) Laurano, R.; Boffito, M.; Cassino, C.; Midei, L.; Pappalardo, R.; Chiono, V.; Ciardelli, G. Thiol-Ene Photo-Click Hydrogels with Tunable Mechanical Properties Resulting from the Exposure of Different -Ene Moieties through a Green Chemistry. *Materials* **2023**, *16* (5), No. 2024.
(28) Torchio, A.; Boffito, M.; Gallina, A.; Lavella, M.; Cassino, C.; Ciardelli, G. Supramolecular Hydrogels Based on Custom-Made Poly(Ether Urethane)s and Cyclodextrins as Potential Drug Delivery Vehicles: Design and Characterization. *J. Mater. Chem. B* **2020**, *8* (34), 7696−7712.
(29) Torchio, A.; Cassino, C.; Lavella, M.; Gallina, A.; Stefani, A.; Boffito, M.; Ciardelli, G. Injectable Supramolecular Hydrogels Based on Custom-Made Poly(Ether Urethane)s and α-Cyclodextrins as Efficient Delivery Vehicles of Curcumin. *Mater. Sci. Eng., C* **2021**, *127* (May), No. 112194.
(30) Boffito, M.; Torchio, A.; Tonda-Turo, C.; Laurano, R.; Gisbert-Garzarán, M.; Berkmann, J. C.; Cassino, C.; Manzano, M.; Duda, G. N.; Vallet-Regí, M.; Schmidt-Bleek, K.; Ciardelli, G. Hybrid Injectable Sol-Gel Systems Based on Thermo-Sensitive Polyurethane Hydrogels Carrying PH-Sensitive Mesoporous Silica Nanoparticles for the Controlled and Triggered Release of Therapeutic Agents. *Front. Bioeng. Biotechnol.* **2020**, *8* (May), 1−24.
(31) Laurano, R.; Cassino, C.; Ciardelli, G.; Chiono, V.; Boffito, M. Polyurethane-Based Thiomers: A New Multifunctional Copolymer Platform for Biomedical Applications. *React. Funct. Polym.* **2020**, *146* (August 2019), No. 104413.
(32) Rahmani, S.; Barzegar, M. One-Pot Synthesis of Dibenzaldehyde-Terminated Poly(Ethylene Glycol) for Preparation of Dynamic Chitosan-Based Amphiphilic Hydrogels. *Polym. Bull.* **2021**, *78* (6), 2887−2909.
(33) Trathnigg, B. Size-Exclusion Chromatography of Polymers. In *Encyclopedia of Analytical Chemistry*; Meyers, R. A., Ed.; Jonh Wiley & Sons Ltd.: Chichester, 2000; pp 8008−8034.
(34) Shivhare, R.; Danao, K.; Nandurkar, D.; Rokde, V.; Ingole, A.; Warokar, A.; Mahajan, U. Schiff Base as Multifaceted Bioactive Core; Akitsu, T., Ed.; IntechOpen: Rijeka, 2022 DOI: 10.5772/intechopen.108387 (Chapter 6).
(35) Wu, Y.; Yuan, L.; Sheng, N. a.; Gu, Z. q.; Feng, W. h.; Yin, H. y.; Morsi, Y.; Mo, X. m. A Soft Tissue Adhesive Based on Aldehyde-Sodium Alginate and Amino-Carboxymethyl Chitosan Preparation through the Schiff Reaction. *Front. Mater. Sci.* **2017**, *11* (3), 215−222.
(36) Qu, J.; Zhao, X.; Ma, P. X.; Guo, B. PH-Responsive Self-Healing Injectable Hydrogel Based on N-Carboxyethyl Chitosan for Hepatocellular Carcinoma Therapy. *Acta Biomater.* **2017**, *58*, 168−180.
(37) Lee, S. H.; Shin, S. R.; Lee, D. S. Self-Healing of Cross-Linked PU via Dual-Dynamic Covalent Bonds of a Schiff Base from Cystine and Vanillin. *Mater. Des.* **2019**, *172*, No. 107774.
(38) Zhou, Z. B.; Tian, P. J.; Yao, J.; Lu, Y.; Qi, Q. Y.; Zhao, X. Toward Azo-Linked Covalent Organic Frameworks by Developing Linkage Chemistry via Linker Exchange. *Nat. Commun.* **2022**, *13* (1), No. 2180, DOI: 10.1038/s41467-022-29814-3.
(39) Martínez, R. F.; Úvalos, M.; Babiano, R.; Cintas, P.; Jiménez, J. L.; Light, M. E.; Palacios, J. C. Schiff Bases from TRIS and Ortho-Hydroxyarenecarbaldehydes: Structures and Tautomeric Equilibria in the Solid State and in Solution. *Eur. J. Org. Chem.* **2011**, *2011* (17), 3137−3145.
(40) Hu, X.; Jazani, A. M.; Oh, J. K. Recent Advances in Development of Imine-Based Acid-Degradable Polymeric Nanoassemblies for Intracellular Drug Delivery. *Polymer* **2021**, *230* (May), No. 124024.
(41) Gu, J.; Cheng, W. P.; Liu, J.; Lo, S. Y.; Smith, D.; Qu, X.; Yang, Z. PH-Triggered Reversible "Stealth" Polycationic Micelles. *Biomacromolecules* **2008**, *9* (1), 255−262.
(42) Lei, Y.; Ouyang, H.; Peng, W.; Yu, X.; Jin, L.; Li, S. Effect of NaCl on the Rheological, Structural, and Gelling Properties of Walnut Protein Isolate-κ-Carrageenan Composite Gels. *Gels* **2022**, *8* (5), No. 259.
(43) Mawad, D.; Odell, R.; Poole-Warren, L. A. Network Structure and Macromolecular Drug Release from Poly(Vinyl Alcohol) Hydrogels Fabricated via Two Crosslinking Strategies. *Int. J. Pharm.* **2009**, *366* (1−2), 31−37.
(44) Feng, W.; Wang, Z. Tailoring the Swelling-Shrinkable Behavior of Hydrogels for Biomedical Applications. *Adv. Sci.* **2023**, *10*, 1−41.

https://doi.org/10.1021/acsomega.4c03157
ACS Omega 2024, 9, 45774−45788